A Novel Self-Correction Method for Linear Displacement Measurement Based on 2-D Synthesis Mechanism

Hai Yu, Qiuhua Wan, and Changhai Zhao

***Abstract*— With increased range, the accuracy of longer-range linear displacement measurement is difficult to guarantee. According to the analysis, it is inevitable that there will be a certain margin between the direction of the calibration grating and the direction of the reading head, which will impact the longer-range linear displacement measurement. In order to eliminate this measurement error, a self-correction method based on 2-D synthesis is herein proposed. First, we describe the principle of absolute linear displacement measurement based on image recognition. Then, the error model is established, which caused by the included angle between the calibration grating and the reading head. Third, a method is proposed for obtaining the vertical offset of the calibration grating by using the vertical image sensor. Finally, we reach an error self-correction method based on 2-D synthesis. In order to test the feasibility of the proposed method, a linear displacement measuring device with a range of 200 mm was developed. After experiment, the maximum absolute error was reduced from 4.34 to 2.03 μm with the proposed error correction in the long range of 200 mm. The proposed algorithm does not depend on the assembly and installation position, and can realize self-correction of errors. So the method could lay the groundwork for improving larger range linear displacement measurement technology.**

***Index Terms*— 2-D displacement synthesis, absolute linear displacement measurement, error self-correction, image recognition algorithm, vertical offset acquisition.**

I. Introduction

With the development of science and technology, the requirements of displacement feedback technology in numerical control systems have become more strict. The field demands higher resolution, higher accuracy, and higher reliability. At present, the mainstream measurement mechanisms for displacement measurement include optical grating, magnetic grating, capacitive grating, and time grating. In the studies on capacitive grating, Anandan and George [1] proposed a wide-range capacitive sensor for linear and angular displacement measurement. Yu et al. [2] proposed a high-precision absolute angular-displacement capacitive sensor using three-stage time-grating in conjunction with a remodulation scheme. In the studies on time grating, Chen et al. [3] proposed a long-range time-grating sensor for displacement measurement and achieved nanometer accuracy. In the studies on magnetic grating, Park et al. [4] and Nguyen et al. [5] tackled high-precision magnetic grating in their studies. In addition, the optical grating displacement measurement technology is widely used due to its strong anti-interference feature, simple structure, and ability to easily perform large-range measurements. In optical grating of studies, effectively correcting the error is a key content, mainly contain: Ye et al. [6] proposed a precise phase demodulation algorithm, and achieved high measurement resolution and accuracy. Tan and Tang [7] proposed a method of online correction of measurement signals using a radial basis function. Lu and Trumper [8] proposed an automatic correction time measurement dynamic reverse (TDR) method for angular displacement measurement. Watanabe et al. [9] proposed an error calibration method with five reading heads evenly distributed in the circumference. Probst [10] proposed an error compensation method based on eight reading heads. However, in the measurement of optical grating, the error compensation is the most accurate method. It is of great significance to study the error compensation method.

A new optical grating measurement technology, the image-type displacement measurement (IDM), has been widely studied. IDM technology first uses image sensors to collect the pattern of lines on the grating and achieves coding value recognition through a digital image processing algorithm. It then performs high-resolution measurement using the sub-pixel displacement subdivision algorithm [11], [12], [13]. Therefore, the IDM technology is a key focus for next generation high-performance linear displacement measurement studies. According to previous study, the IDM technology has the following advantages:

1) "Higher fault tolerance." Using image recognition algorithms, the decoding and subdivision of IDM can be realized only by a single code channel, so as to ensure measurement reliability [14].
2) "Stronger robustness." IDM uses a full digital processing algorithm, which can directly perform displacement subdivision through a digital image positioning algorithm, and ensures stable measurement accuracy [15].

Manuscript received 4 August 2022; revised 24 September 2022; accepted 7 October 2022. Date of publication 19 October 2022; date of current version 2 November 2022. This work was supported in part by the National Natural Science Foundation of China under Grant 52075520, in part by the Jilin Scientific and Technological Development Program under Grant 20210201097GX, and in part by the Youth Innovation Promotion Association, Chinese Academy of Sciences under Grant 2022221. The Associate Editor coordinating the review process was Chi-Hung Hwang. *(Corresponding author: Hai Yu.)*

The authors are with the Changchun Institute of Optics, Fine Mechanics and Physics, Chinese Academy of Sciences, Changchun 130033, China (e-mail: yuhai@ciomp.ac.cn).

Digital Object Identifier 10.1109/TIM.2022.3216061

3) "Higher measurement resolution." In IDM, the sub-pixel subdivision algorithm is used to replace the traditional algorithm, so as to perform higher resolution displacement measurement [16].
4) "Easier to achieve high-precision measurement." IDM can simultaneously obtain "gray value information" and "pixel position information," and it is easier to improve its own accuracy through the algorithm [17].

In the research of IDM, Leviton and Frey [18] used area-scan image sensors to receive grating patterns with reference lines and binary symbols and achieved 0.01-μm measurement resolution and 0.2-μm accuracy. Xu et al. [19] proposed superimposing image arrays to form virtual moiré fringes, achieving 0.1-μm resolution and 0.4-μm measurement accuracy. Das et al. [20] proposed a linear displacement measurement method based on a gray gradient pattern, leading to a measurement resolution of 1 mm. Lashmanov et al. [21] used the camera to collect and measure the scale ruler with scale line, and achieved 0.02-μm resolution and 1.65-μm measurement accuracy. Mu et al. [22] used CMOS image sensors to recognize single code channel coding, and performed 20-bit coding recognition. In the error compensation of IDM, Yuan et al. [23] proposed a high-precision subdivision algorithm with robust performance that can improve measurement accuracy. Yu et al. [24] proposed a method to realize high-precision error compensation on low-density metal circular grating. At the same time, Yu et al. [25] also proposed a high-precision angular displacement measurement method based on three image sensors.

Among many research works, there are few error compensation methods for linear IDM based on the image recognition method. The research on error compensation based on the flexibility of image recognition needs further research.

In 2021, we developed a displacement measurement technology based on an image recognition algorithm and proposed a linear IDM method based on grating projection imaging [26]. In addition, in 2022, we proposed a depth fusion algorithm to improve the accuracy of displacement measurement and achieved a measurement standard deviation of 1.26 μm within a straight-line range of 250 mm [17]. According to our previous study, when the linear displacement measurement range increases, the measurement accuracy becomes more difficult to ensure. Therefore, there is a contradiction between the range and the measurement accuracy. It can then be deduced that in the long-range IDM, the movement direction of the reading head is not parallel to the direction of the calibration grating. This will lead to large errors in the long-range IDM. Especially for the long-range linear IDM, very few studies attempted to improve the measurement accuracy. Therefore, this article studies the self-correction method in linear IDM, and proposes a self-correction method based on 2-D displacement synthesis over a long range.

The remainder of this article is organized as follows. Section II introduces the principle of linear IDM. Section III presents the developed error model and error self-correction method. Section IV details the proposed implementation method of error compensation. Section V presents the simulation of the proposed algorithm. Section VI shows the experimental verification. Finally, the conclusion is drawn in Section VII.

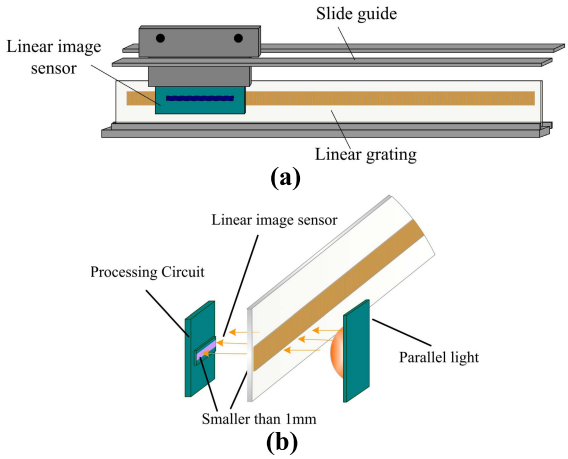

Fig. 1. Linear IDM measurement. (a) Schematic of linear IDM measurement. (b) Principle of grating projection imaging.

II. Principle of Linear IDM

A. Linear Displacement Coding

IDM is a new displacement measurement technology that uses image recognition methods to perform linear displacement measurements. In the previous study, in order to perform the linear displacement measurement without a lens, a method based on grating projection imaging was proposed [27] (Fig. 1).

When working, the light emitted by the parallel light source shines on the scale grating, and the coded line pattern on the grating is mapped onto the linear-scan image sensor. In order to improve the projection imaging quality, the distance between the image sensor and the scale grating is set to almost 1 mm. After the coded line pattern is collected by the image sensor, the "decoding" and "subdivision" operations are carried out to measure the absolute linear displacement through the same code track.

The scale grating contains N coding lines for displacement measurement, while the spacing of all the coding lines is the same. In order to perform an absolute measurement, the "wide" coding line and "narrow" line are set to represent coding elements "1" and "0," respectively. Fig. 2 shows the line pattern on the scale grating when the number of absolute value coding bits is $n = 9$ bit ($N \leq 2^n$).

The coding element represented by the ith coding line is set to d_i. Since the binary digits of N are n (assume $n = 9$ bit), adjacent n coding elements form a coding group, including the ith coding element and the $n-1$ adjacent coding elements after. Each coding group is expressed as $\{D_i\} = \{d_i, d_{i+1}, \ldots, d_{i+n-2}, d_{i+n-1}\}$. When the linear-scan image sensor moves along the grating direction, the recognized coding group will change from $\{D_i\} = \{d_i, d_{i+1}, \ldots, d_{i+n-2}, d_{i+n-1}\}$ to $\{D_{i+1}\} = \{d_{i+1}, d_{i+2}, \ldots, d_{i+n-1}, d_{i+n}\}$, forming a new coding group, as shown in Fig. 2.

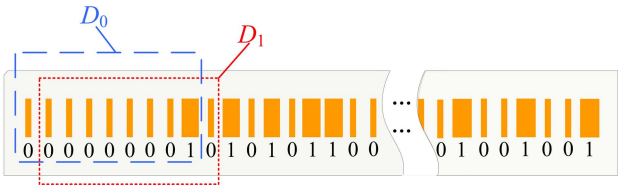

Fig. 2. Principle of absolute coding (9-bit coding).

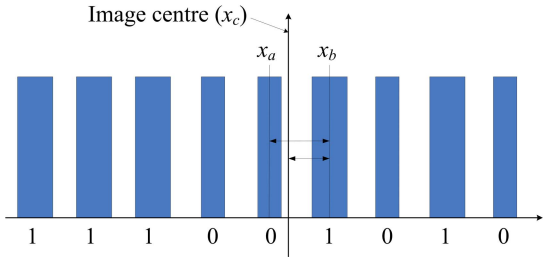

Fig. 3. Image collected by linear scan image sensor.

In Fig. 2, the initial coding group when $i = 0$ is set to $\{D_0\} = \{d_0, d_1, \ldots, d_9\} = \{0, 0, 0, 0, 0, 0, 0, 0, 1\}$ (as the first group of coding). When the image sensor moves to the right, the recognized coding group will change from $\{D_0\}$ to $\{D_1\} = \{0, 0, 0, 0, 0, 0, 0, 1, 0\}$. Moving the image sensor N times will lead to N groups of codes $\{D_0\}$–$\{D_{N-1}\}$.

In order to make each group of codes $\{D_i\}$ unique, the value of each bit of code element d_i after $i = 9$ is calculated by the "XOR" operation of the first n code element values

$$d_i = k_1 d_{i-1} \oplus k_2 d_{i-2} \oplus \cdots \oplus k_n d_{i-n}, \quad (i = 10 \sim N) \quad (1)$$

where "$\oplus$" represents the XOR operation and $k_1 - k_n$ is the coefficient of the n-bit coded element XOR operation ("0" or "1").

By reasonably selecting the value of the coefficient k_1–k_n, up to 2^n different code groups can be obtained. Since there are only N codes in the range, the first N code groups are considered ($N < 2^n$). When $n = 9$ bit, the calculation of the coding element is given by

$$d_i = d_{i-1} \oplus d_{i-6}. \quad (2)$$

Set A is the decoding value, and the decoding value of each group of codes is $A = i$ according to the relationship between $\{D_i\}$ and i.

B. Subdivision Principle of Linear Displacement

In order to improve the resolution of linear IDM, it is necessary to further develop subdivision operations between the adjacent coding lines. The scale grating with the range of L contains N coding lines. At this time, the spacing of the coding lines is given by

$$\Delta L = \frac{L}{N-1}. \quad (3)$$

The mapping pattern on the linear-scan image sensor, in a certain acquisition, is shown in Fig. 3.

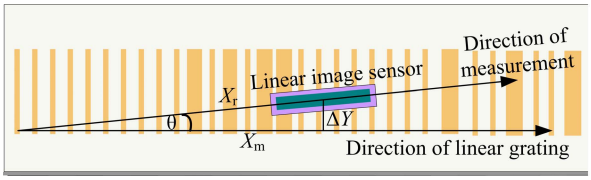

Fig. 4. Schematic of the range error of image measurement.

The coding value is determined according to the width of the coding line in the collected image. The "wide" coding line represents "1" and the "narrow" line represents "0." Therefore, the coding value in Fig. 3 is "111 001 010." In addition, the coding lines on both sides of the image center point will be located and calculated to obtain x_a and x_b. The subdivision calculation will then be carried out according to (4). Thus, the subdivision value B can be obtained

$$B = \Delta L \cdot \frac{x_b - x_c}{x_b - x_a} \quad (4)$$

where x_c represents the position of the image center.

Finally, after decoding and subdivision, the results of linear IDM are

$$X_m = A \cdot \Delta L + B. \quad (5)$$

III. Error Analysis in Linear IDM

A. Error Model Establishment

Because the IDM technology uses the full digital subdivision method, it is not affected by signal amplitude, phase change, and other factors. The measurement accuracy is high in the subdivision cycle. The error within the range (i.e., cosine error) is one of the main errors in linear IDM.

Due to factors such as grating pattern printing, machining, installation, and commissioning, the image sensor moving direction is not parallel to the grating direction, which will make the measured values smaller than the real ones. The principle of error generation is shown in Fig. 4.

In Fig. 4, the included angle between the image sensor direction and the grating extension direction is θ. The actual displacement value and the measured value are set to X_r and X_m, respectively. The error value in Fig. 4 can then be expressed as

$$e = X_r - X_m = (1 - \cos\theta) X_r. \quad (6)$$

Equation (6) presents the error model of linear IDM. It can be seen that the error will gradually increase with the increase of the actual measurement range X_r. When X_r is large, a small included angle will produce a large error.

B. Error Self-Correction Algorithm

According to the error model in (6), if the vertical offset ΔY in Fig. 4 can be obtained, then according to the error synthesis principle, the real measured value can be reached

$$X_r = \sqrt{X_m^2 + \Delta Y^2}. \quad (7)$$

Note that the "square root operation" in (7) makes the microprocessor calculation slow and wastes processor

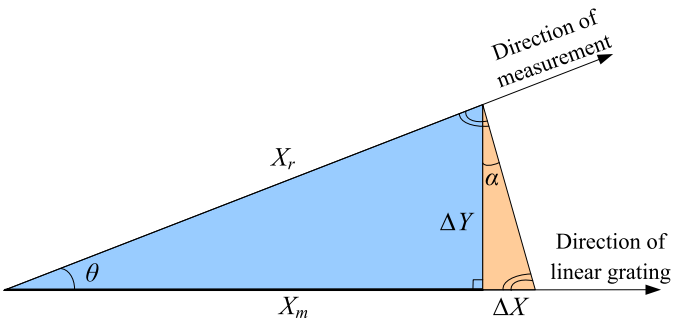

Fig. 5. Schematic of the summation algorithm.

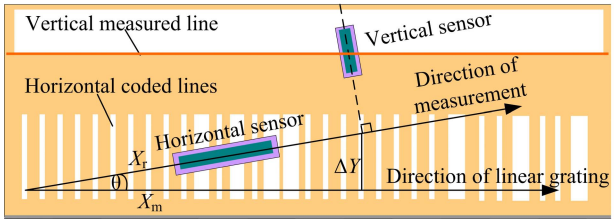

Fig. 6. Vertical displacement acquisition method.

resources. Therefore, (7) should be modified. Assuming that the actual displacement X_r is equal to the sum of the measured value X_m and a variable ΔX, the actual measured value X_r can be expressed as

$$X_r = X_m + \Delta X. \tag{8}$$

Equation (8) is a "summation algorithm" of error synthesis. Consequently, the relationship between ΔX and the actual displacement measurement value X_r is shown in Fig. 5.

In Fig. 5, ΔX is the extension line of the side where X_m is located. According to (8), $X_m + \Delta X = X_r$. In addition, if the ratio of $\tan\alpha$ to $\tan\theta$ is k, then $k{\cdot}\tan\theta = \tan\alpha$. According to the ratio relationship, a relationship can be reached where $k{\cdot}\Delta Y/X_m = \Delta X/\Delta Y$ such that $\Delta X = k{\cdot}\Delta Y^2/X_m$. In this case, X_r can be approximately expressed as

$$X_r \approx X_m + \Delta X = X_m + k\left(\Delta Y^2/X_m\right). \tag{9}$$

If the coefficient k in (9) is reasonably selected, (9) can approach the real measured value X_r. It can also be deduced by simulation that when θ gradually decreases, k tends to be close to 0.5 (we will demonstrate it in Section V). The proposed compensation model of error is given by

$$X_r = X_m + 0.5\left(\Delta Y^2/X_m\right). \tag{10}$$

IV. Vertical Displacement Method

According to the error self-correction model in (10), in the process of error correction, it is necessary to obtain the value of vertical displacement ΔY. Therefore, it is necessary to set a "vertical measured line" across the whole range on the calibration grating. The upper area of the "vertical measured line" is transparent and the lower area is opaque, as shown in Fig. 6.

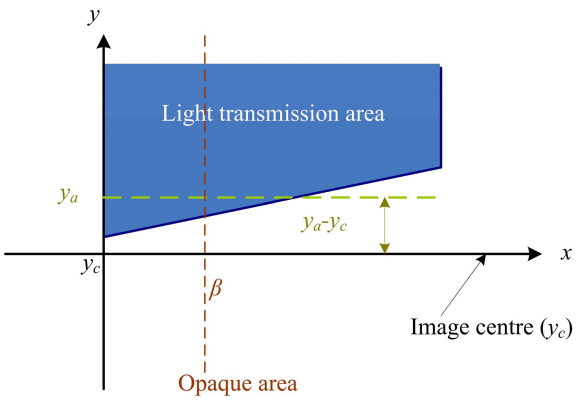

Fig. 7. Gray value curve of grating edge.

In order to obtain the displacement, the horizontal and vertical sensors are set to obtain the horizontal and vertical displacements, respectively.

In the used coordinate system, the pixel position of the vertical sensor is the y-axis (denoted by y), and the gray value is considered as the x-axis [denoted by $x(y)$]. The image information collected by the vertical sensor is shown in Fig. 7.

Since the areas on both sides of the "vertical measured line" are, respectively, "light transmitting" and "light impermeable," the pixel gray value collected in Fig. 7 also includes light transmitting area and light impermeable area. In order to calculate a split point between the light transmission area and the light tight area, the threshold value is set to β, 50 pixels $x(y)$ larger than the threshold value β are taken at the boundary of the light transmission area, and the centroid position of these 50 pixels is calculated, as shown in the following equation:

$$y_a = \frac{\sum_{x(y)>\beta}^{50} x^2(y) \cdot y}{\sum_{x(y)>\beta}^{50} x^2(y)}. \tag{11}$$

In general, let β = (pixel_max-pixel_min) $\times$ 0.3, where, pixel_ max is the maximum gray value in the image and pixel_min is the minimum gray value in the image.

Let the center point of the vertical image sensor image be y_c. The offset between the dividing point y_a and the image center point y_c is then $y_c - y_a$. In order to facilitate the 2-D synthesis algorithm, the offset is mapped to the same $x_b - x_a$ range (ΔL) as in (4). This allows calculating the relative displacement value of the vertical displacement

$$Y_m = \Delta L \cdot \left|\frac{y_a - y_c}{x_b - x_a}\right| \tag{12}$$

where ΔL represents the mapping value of the vertical offset to make it the same as the horizontal direction. Limited by sensor acquisition noise and sub-pixel subdivision limit, the value of ΔL cannot be infinite. Generally, we will determine the value of ΔL through experiments.

After obtaining the edge position Y_m, the error self-correction process based on 2-D displacement synthesis is shown in Fig. 8.

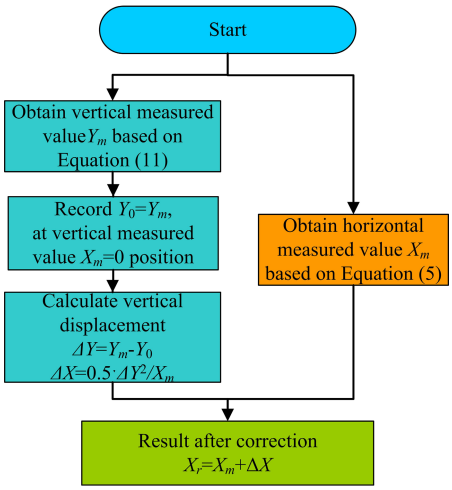

Fig. 8. Flowchart of the error self-correction algorithm.

The specific process is summarized as follows:

1) The horizontal image sensor is used to obtain the measured value X_m of the calibration grating through the image recognition algorithm (5).
2) The vertical offset Y_m of the calibration grating is calculated by the vertical image sensor.
3) When the horizontal measurement value X_m is at the zero position, the initial vertical position $Y_0 = Y_m|_{Xm} = 0$ is recorded by the vertical sensor and stored.
4) The measured value is corrected (the edge position recognized by the vertical sensor at any position is Y_m and the change measured by the vertical sensor is ΔY) as follows:

$$\Delta Y = Y_m - Y_0. \tag{13}$$

5) The vertical offset ΔY is brought into (10) to perform the error compensation operation of the "summation algorithm"

$$X_r = X_m + \Delta X = X_m + \frac{0.5 \cdot (Y_m - Y_0)^2}{X_m}. \tag{14}$$

In (14), we use both the horizontal displacement sensor and the vertical displacement sensor. The displacement obtained by the horizontal displacement sensor is absolute, and its zero position is fixed. Therefore, the vertical displacement sensor will always be "clear to 0" at the horizontal zero position. This method makes the installation state of the reading head not affect the error calibration effect in (14), thus greatly improving the robustness of error self-correction.

V. Simulation

A. Numerical Simulation of Coefficient k

In order to analyze the feasibility of the coefficient k in the proposed error compensation algorithm, the variation range of the included angle θ between the measurement direction and grating direction is set to $0 \sim 3°$. The horizontal measurement value is set to X_m = (0–1000 mm) and the vertical displacement is set to $\Delta Y = \tan(\theta) \cdot X_m$. The real measured value can be calculated as $X_r = (X_m^2 + \Delta Y^2)^{1/2}$.

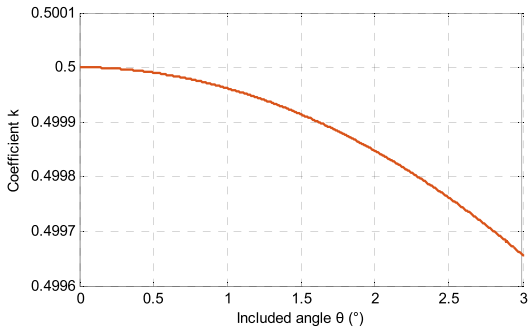

Fig. 9. Variation of k function of θ.

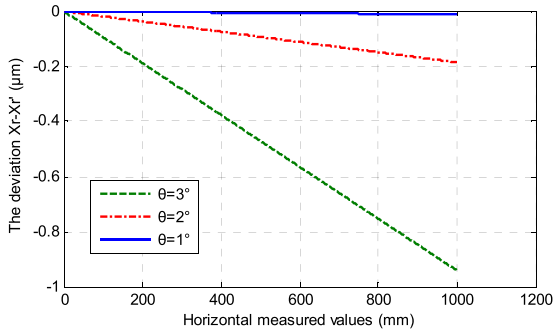

Fig. 10. Error simulation curve.

According to (10), the expression of the coefficient is $k = (X_r - X_m)/(\Delta Y^2/X_m)$. The simulated curve of the variation of k function of θ is shown in Fig. 9.

It can be seen that when θ decreases, the value of k gradually approaches 0.5. In practical measurement, the actual installation of the calibration grating will make the included angle very small. In addition, it is feasible to make the coefficient k equal to 0.5 in practical applications.

B. Simulation of Measurement Error

Let the angle be $\theta = 0°$–$3°$. The compensation effect of the summation error compensation algorithm is then simulated. The variation range of horizontal displacement X_m is set to 0–1000 mm, and the vertical displacement of $\Delta Y = \tan(\theta) \cdot X_m$, is obtained. The error $X_r - X'_r$ curve between the proposed result $X'_r = X_m + 0.5 \cdot (\Delta Y^2/X_m)$ and the real displacement value $X_r = (X_m^2 + \Delta Y^2)^{1/2}$ is shown in Fig. 10.

It can be seen from Fig. 10 that when the included angle θ gradually increases, the maximum deviation of the proposed error correction algorithm also gradually increases. However, it can still be seen that when $\theta \leq 3°$, the difference $|X'_r - X_r|$ between the summation algorithm result and the real value in the range of 0–1000 mm is less than 1 μm. The error is small and high-precision error-correction can be achieved. Therefore, it can be concluded by simulation that when the included angle θ between the scale grating and the moving direction of the image sensor is small, the error correction method of the proposed "summation algorithm" is feasible.

VI. Experiment

A. Experimental Device Design

In order to test the performance of the proposed method, a linear IDM device was designed and tested [Fig. 11(a)].

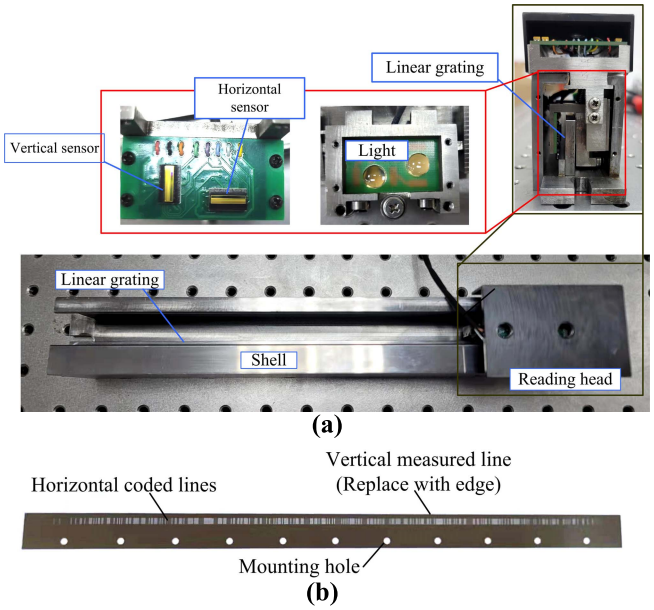

Fig. 11. Experimental device. The experimental equipment is made of stainless steel (it includes grating ruler and shell). (a) Composition of the measuring device. (b) Used metal scale grating.

Fig. 11(a) includes reading head, shell, and scale grating. The reading head includes horizontal and vertical image sensors, as well as parallel light sources. When the reading head moves, the linear-scan image sensor continuously scans the pattern on the scale grating to measure the linear displacement.

In Fig. 11, the sensor we use is a CCD image sensor with 1×320 photosensitive pixels, and the distance between adjacent pixels is 0.254 μm. The length of the total photosensitive area was 8.128 mm. Through the acquisition of the digital-to-analog converter, the gray value range of each pixel is quantized to 0–65535.

The scale grating used in the experiment is made of metal, which is engraved with transparent horizontal coding lines, as shown in Fig. 11(b). The effective range of the designed scale grating is 200 mm, and the number of horizontal line coding bits is $n = 9$ bit. In Fig. 11(b), the spacing of horizontal lines is $\Delta L = 0.5$ mm. In our calculation, we mapped the measured value ΔL to the range of 250 000. That is to say, in order to achieve the acquisition of digital displacement, we quantize ΔL to a value 250 000. By quantifying ΔL as 250 000, we achieved a 250 000-fold displacement subdivision, so that the resolution of vertical displacement measurement is $\Delta L/250\,000 = 0.5$ mm/250 000 $= 0.002$ μm.

In order to obtain the vertical displacement, the upper edge of the scale grating is used as the "vertical measured line" in the experiment. Thus, the "vertical sensor" is used to detect the position of the upper edge of the scale grating to obtain the vertical displacement.

B. Horizontal Measurement Error Test

Without using the correction algorithm proposed in (14), the horizontal coding lines are used to directly test the error of linear displacement. The laser interferometer is used to align the mirror installed on the reading head. The measurement error is then obtained by comparing the measurement values produced by the laser interferometer and the experimental device. The experimental principle is shown in Fig. 12.

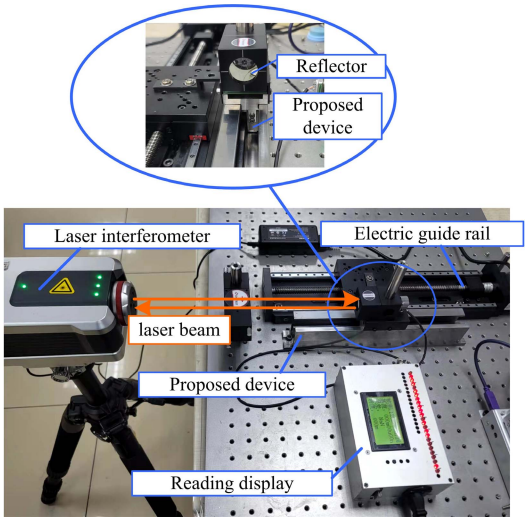

Fig. 12. Schematic of the experiment.

During the error test, the mirror of the laser interferometer is placed as close as possible to the moving axis of the experimental device so as to minimize the influence of the "Abbe error." At the same time, the angle of the laser interferometer is carefully adjusted to collimate the emitted laser with the reflected light, and therefore minimize the "cosine error" introduced by the laser interferometer.

The measurement resolution of the used laser interferometer is 1 nm, and the linearity measurement accuracy is 0.5 ppm (0 °C–40 °C). The room temperature of the experimental equipment is 23 °C, and the humidity is 40%.

The experimental device shown in Fig. 12 is used to obtain the error value without error compensation. During measurement, the measured value is recorded approximately every 10 mm. The values of the laser interferometer and the measured values of the experimental device are shown in Table I. The error data of the proposed device are obtained by calculating the differences between the measured values and the laser interferometer values.

It can be seen that there are some errors caused by the included angle between the moving direction and the calibration grating direction. The error in Table I gradually increases with the increase of the measurement range. The maximum absolute error is 4.34 μm.

C. Error Compensation Algorithm Test

The measurement algorithm proposed in (14) is used for error compensation testing. A vertical sensor is used to measure the vertical displacement. Equation (14) contains the ratio operation of $(y_c - y_a)$ and $(x_b - x_a)$, where, the mapping spacing of $(x_b - x_a)$ is $\Delta L = 0.5$ mm.

The change of the vertical offset value ΔY, within the range of 0–200 mm, is shown in Fig. 13(a). It can be seen that with the increase of the measurement range, the vertical offset also

TABLE I
MEASURED VALUE WHEN ONLY USING A HORIZONTAL SENSOR

No.	Interferometer values(μm)	Proposed device values(μm)	Errors(μm)
1	0	0	0
2	10054.35	10053.07	-1.28
3	20057.78	20057.13	-0.65
4	30059.12	30058.57	-0.55
5	40063.8	40061.94	-1.86
6	50061.07	50058.75	-2.32
7	60063.62	60062.35	-1.27
8	70060.04	70058.05	-1.99
9	80070.12	80069.02	-1.1
10	90066.77	90064.34	-2.43
11	100077.56	100074.43	-3.13
12	110075.37	110073.31	-3.06
13	120087.61	120084.66	-2.95
14	130086.13	130084.52	-1.61
15	140096.8	140094.78	-2.02
16	150094.91	150092.52	-2.39
17	160101.92	160098.65	-3.27
18	170118.8	170116.67	-2.13
19	180138.2	180134.67	-3.53
20	190150.37	190147.14	-3.23
21	200156.09	200151.75	-4.34

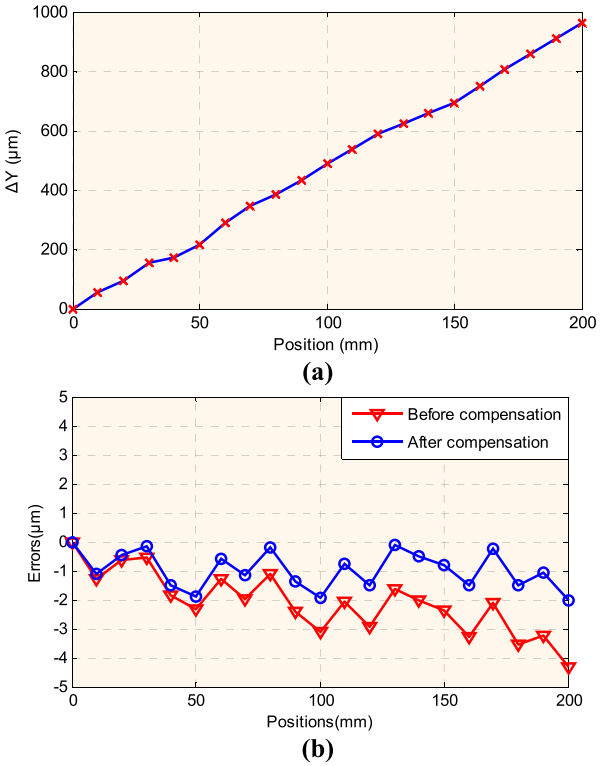

Fig. 13. Experimental results. (a) Vertical displacement numerical curve. (b) Comparison before and after error compensation.

gradually increases. The vertical offset value ΔY in Fig. 13(a) will lead to a large error.

The obtained vertical displacement data are brought into (14) to produce error correction. For comparison, the error curve without ΔY value (before compensation) is shown as the red curve in Fig. 13(b). The error curve after adding ΔY value (after compensation) is shown as the blue curve in Fig. 13(b).

It can be seen that before error compensation, the maximum absolute value of measurement error is 4.34 μm. After the proposed self-correction method, the maximum absolute value of the measurement error is 2.03 μm. It can be clearly deduced that the error value is reduced by the proposed error self-correction method.

D. Analysis of Experimental Results

Through the comparative observation of the error correction curve in Fig. 13(b), it can be seen that there is still a certain fluctuation in the corrected error curve. Four main factors exist as follows:

1) In the linear measurement, the sliding guide rail cannot achieve the alignment and smoothness of the ideal state. The bearing roller on the reading head will necessarily fluctuate when sliding. The relative position between the image sensor and the scale grating changes, which results in inconsistent measurement error.
2) The edge detection of scale grating is the main approach for obtaining vertical displacement in the experiment. The irregular edge of the metallic scale grating will also modulate the effect of error correction. If the calibration grating is made of glass, a more accurate vertical measured line can be printed on the glass to improve the measurement of vertical displacement.
3) In the production of metallic scale grating, the marking error of the coding line pattern is also a factor affecting the measurement accuracy.
4) The proposed error correction algorithm performs well when the included angle θ is small ($\theta \leq 3°$). When θ is large, the error correction effect will also decrease, but it can still achieve a certain degree of correction.

In addition, when the measurement range is larger than the range in our experiment (200 mm), the proposed method can still accurately obtain the vertical displacement. Meanwhile, according to the cosine error model in (6), the measurement error will be gradually amplified with the increase of the measurement range. Therefore, when the vertical displacement can be obtained accurately, the proposed measurement method will reduce the measurement error more effectively in a large range.

VII. CONCLUSION

IDM is a new technology used to measure absolute linear displacement. Due to its high fault tolerance, strong adaptability, and easiness of achieving a high-resolution measurement, it has become an important technology for the future of photoelectric displacement measurement. Errors exist in the measurement of linear displacement. They are mainly caused by the included angle between the reading head direction and grating direction. This greatly affects the measurement accuracy of long-range linear displacement. In the process of studying the linear IDM, this article proposes a novel error self-correction method for linear displacement measurement based on 2-D displacement synthesis, which is verified by the experimental device.

This article first introduces the principle of linear IDM. An error self-correction method based on two-dimensional displacement synthesis is then proposed. Finally, simulation and experiments are carried out. The obtained results show that the proposed algorithm can significantly reduce the measurement error caused by the included angle. A linear displacement measuring device with a range of 200 mm was then designed to verify the proposed method. Consequently, the maximum absolute error was reduced from 4.34 to 2.03 μm in the range of 200 mm.

The proposed error self-correction algorithm can effectively eliminate the error in linear IDM, which lays a theoretical foundation for the studies on high-precision linear displacement measurement technology.

REFERENCES

[1] N. Anandan and B. George, "A wide-range capacitive sensor for linear and angular displacement measurement," *IEEE Trans. Ind. Electron.*, vol. 64, no. 7, pp. 5728–5737, Jul. 2017.

[2] Z. Yu, K. Peng, X. Liu, Z. Chen, and Y. Huang, "A high-precision absolute angular-displacement capacitive sensor using three-stage time-grating in conjunction with a remodulation scheme," *IEEE Trans. Ind. Electron.*, vol. 66, no. 9, pp. 7376–7385, Sep. 2019.

[3] Z. Chen, H. Pu, X. Liu, D. Peng, and Z. Yu, "A time-grating sensor for displacement measurement with long range and nanometer accuracy," *IEEE Trans. Instrum Meas.*, vol. 64, no. 11, pp. 3105–3115, Nov. 2015.

[4] J. W. Park, H. X. Nguyen, T. N.-C. Tran, and J. W. Jeon, "A linear compensation method for improving the accuracy of an absolute multipolar magnetic encoder," *IEEE Access*, vol. 9, pp. 19127–19138, 2021.

[5] T. H. Nguyen et al., "An effective method to improve the accuracy of a Vernier-type absolute magnetic encoder," *IEEE Trans. Ind. Electron.*, vol. 68, no. 8, pp. 7330–7340, Jun. 2021.

[6] G. Ye, G. Zhao, H. Liu, and B. Lu, "Precise phase demodulation algorithm for sinusoidal encoders and resolvers," *IEEE Trans. Ind. Electron.*, vol. 67, no. 10, pp. 8778–8787, Oct. 2020.

[7] K. K. Tan and K.-Z. Tang, "Adaptive online correction and interpolation of quadrature encoder signals using radial basis functions," *IEEE Trans. Control Syst. Technol.*, vol. 13, no. 3, pp. 370–377, May 2005.

[8] X. D. Lu and D. L. Trumper, "Self-calibration of on-axis rotary encoders," *CIRP Ann. Manuf. Technol.*, vol. 56, no. 1, pp. 499–504, Jun. 2009.

[9] T. Watanabe, T. Masuda, M. Kajitani, H. Fujimoto, and K. Nakayama, "Automatic high precision calibration system for rotary encoder," *J. Jpn. Soc. Precis. Eng.*, vol. 67, no. 7, pp. 1091–1095, 2001.

[10] R. Probst, "Self-calibration of divided circles on the basis of a prime factor algorithm," *Meas. Sci. Technol.*, vol. 19, no. 1, Jan. 2008, Art. no. 015101.

[11] T. Dziwinski, "A novel approach of an absolute encoder coding pattern," *IEEE Sensors J.*, vol. 15, no. 1, pp. 397–401, Jan. 2015.

[12] S. Das, T. S. Sarkar, B. Chakraborty, and H. S. Dutta, "A simple approach to design a binary coded absolute shaft encoder," *IEEE Sensor J.*, vol. 16, no. 8, pp. 2300–2305, Apr. 2016.

[13] Y. Sugiyam et al., "A 3.2 kHz 14-bit optical absolute rotary encoder with a CMOS profile sensor," *IEEE Sensors J.*, vol. 8, no. 8, pp. 1430–1436, Jul. 2008.

[14] H. Yu, Q. Wan, X. Lu, Y. Du, and S. Yang, "Small-size, high-resolution angular displacement measurement technology based on an imaging detector," *Appl. Opt.*, vol. 56, no. 3, pp. 755–760, 2017.

[15] H. Yu, Q. Wan, X. Lu, C. Zhao, and Y. Du, "A robust sub-pixel subdivision algorithm for image-type angular displacement measurement," *Opt. Laser. Eng*, vol. 100, pp. 234–238, Jan. 2018.

[16] H. Yu, X. Jia, Q. Wan, C. Zhao, and Y. Sun, "High-resolution angular measurement arithmetic based on pixel interpolations," *Measurement*, vol. 149, Jan. 2020, Art. no. 106948.

[17] H. Yu, Q. Wan, X. Lu, Y. Du, and L. Liang, "High-precision displacement measurement algorithm based on a depth fusion of grating projection pattern," *Appl. Opt.*, vol. 61, no. 4, pp. 1049–1056, 2022.

[18] D. B. Leviton and B. J. Frey, "Ultra-high resolution, absolute position sensors for cytostatic applications," *Proc. SPIE*, vol. 4850, pp. 776–787, Mar. 2003.

[19] J. Xu et al., "Virtual Moiré fringe for grating measurement system based on CMOS microscopic imaging," *Proc. SPIE*, vol. 7853, pp. 1–5, Nov. 2010.

[20] S. Das and T. S. Sarkar, "A new method of linear displacement measurement utilizing a grayscale image," *Int. J. Electron. Elect. Eng.*, vol. 1, no. 3, pp. 176–181, 2013.

[21] O. U. Lashmanov et al., "High-precision absolute linear encoder based on a standard calibrated scale," *Measurement*, vol. 123, pp. 226–234, Jul. 2018.

[22] Y. Mu et al., "A 7.4 kHz, 20-bit image encoder with a CMOS linear image sensor," *Opt. Quantum Electron.*, vol. 51, p. 321, Oct. 2019.

[23] P. Yuan, D. Huang, Z. Lei, and C. Xu, "An anti-spot, high-precision subdivision algorithm for linear CCD based single-track absolute encoder," *Measurement*, vol. 137, pp. 143–154, Apr. 2019.

[24] H. Yu, Q. Wan, C. Zhao, Q. Han, and Z. Mu, "Error compensation for low-density circular gratings based on linear image-type angular displacement measurements," *IEEE Trans. Ind. Electron.*, vol. 69, no. 12, pp. 13736–13743, Dec. 2022.

[25] H. Yu, Q. Wan, X. Lu, C. Zhao, and L. Liang, "High precision angular displacement measurement based on self-correcting error compensation of three image sensors," *Appl. Opt.*, vol. 61, no. 1, pp. 287–293, 2022.

[26] H. Yu, Q. Wan, Z. Mu, Y. Du, and L. Lihui, "Novel nano-scale absolute linear displacement measurement based on grating projection imaging," *Measurement*, vol. 182, Sep. 2021, Art. no. 109738.

Hai Yu was born in Jilin, China, in 1987. He received the B.S. degree in electronic information science and technology from Northeast Dianli University, Jilin, in 2009, and the Ph.D. degree in mechanical and electronic engineering from the University of Chinese Academy of Sciences, Beijing, China, in 2014.

He is currently an Associate Researcher with the Research and Development Center for Precision Instruments and Equipment, Changchun Institute of Optics, Fine Mechanics and Physics, Chinese Academy of Sciences (CIOMP), Changchun, China. Since 2017, he has been a Project Leader for several Natural Science Foundation of China (NSFC) and other agency-funded projects. His current research interests include electro-optical displacement precision measurement.

Dr. Yu was elected to the Youth Innovation Promotion Association of the Chinese Academy of Sciences, in 2022.

Qiuhua Wan was born in Jilin, China, in 1962. She received the Ph.D. degree in optical engineering from the University of Chinese Academy of Sciences, Beijing, China, in 2009.

She is currently a Researcher with the Research and Development Center for Precision Instruments and Equipment, Changchun Institute of Optics, Fine Mechanics and Physics, Chinese Academy of Sciences (CIOMP), Changchun. Her current research interest lies in electro-optical displacement precision measurement.

Changhai Zhao was born in Henan, China, in 1980. He received the Ph.D. degree in mechanical and electronic engineering from the University of Chinese Academy of Sciences, Beijing, China, in 2008.

He is currently an Associate Researcher with the Research and Development Center for Precision Instruments and Equipment, Changchun Institute of Optics, Fine Mechanics and Physics, Chinese Academy of Sciences (CIOMP), Changchun, China. His current research interests in electro-optical displacement precision measurement.